PAPER

Novel synthesis and anti-pathogenic properties of ensifentrine and its intermediates against *Pseudomonas aeruginosa*†

Anusree Sajeevan,‡[a] Deepthi Joseph Andrew,‡[a] T. Nalinikanta Patra,‡[b] Adline Princy Solomon [ID] *[a] and Rambabu Dandela*[b]

Chronic obstructive pulmonary disease (COPD) is a progressive respiratory disorder marked by persistent lung inflammation and airway constriction. It presents a formidable global health challenge owing to its high morbidity and mortality rates. It is often aggravated by infections from pathogens such as *Pseudomonas aeruginosa*, a predominant pathogen that accelerates lung function deterioration and triggers frequent exacerbations. Ensifentrine (ENF) exhibits strong anti-inflammatory effects and is a selective dual inhibitor of the enzymes PDE3 and PDE4, which have been reported to be beneficial in treating COPD exacerbation. This study examined the anti-pathogenic activity of ENF against *P. aeruginosa* by adopting an innovative synthetic route. A series of intermediates were synthesized *via* the novel route, optimizing the yield and integrity of ENF. Further investigations to determine the activity of the compound against *P. aeruginosa* involved antibacterial and antibiofilm testing and identification of the potential mechanisms of action. Preliminary results demonstrate that ENF and its intermediate ENF[A] exhibit 50–60% robust biofilm-inhibition and biofilm-eradication effects at remarkably low concentrations of 3.9 μM and 7.9 μM, respectively. Furthermore, ENF disrupts quorum sensing, leading to a 35% reduction in the production of pyoverdine and exopolysaccharide, which are two key virulence factors of *P. aeruginosa*. Importantly, ENF exhibits synergistic activity with ciprofloxacin, further enhancing its antimicrobial efficacy at a concentration of 0.25 μg mL^{-1}. This study focuses on the innovative synthesis of ENF and its promising anti-pathogenic properties, which may make it an effective adjunctive treatment for COPD caused by *P. aeruginosa*.

Introduction

Chronic obstructive pulmonary disease (COPD) is a chronic condition characterized by inflamed bronchioles and narrowed air passages. COPD causes 3.2 million deaths every year, and the number continues to rise. Tobacco smoking and smoking are the primary causes of COPD. Patients affected by COPD experience cough, shortness of breath, and excessive phlegm production, which causes wheezing. These patients are highly prone to various pathogenic bacterial colonization and are at a higher risk of developing severe illness. A major proportion of the disease arises from recurrent exacerbations, which further deteriorate health and worsen outcomes.[1] The progression and

pathogenesis of COPD are caused by significant bacterial infections. Among these pathogenic bacteria, *Pseudomonas aeruginosa*, a Gram-negative, opportunistic microorganism, is the major reason for lower respiratory tract infections because it colonizes in the lungs.[2,3]

The World Health Organization (WHO) classifies *P. aeruginosa* as a priority pathogen in terms of antimicrobial resistance (AMR) owing to its intrinsic resistance mechanisms, where it acquires resistance through horizontal gene transfer and mutations (WHO, 2024). The Centers for Disease Control and Prevention reported that AMR in *P. aeruginosa* contributes to over 32 600 deaths annually in the United States alone. By 2050, the annual deaths caused by AMR-associated infections caused by *P. aeruginosa* are projected to reach about 10 million if the current trends persist.[4] Several reports have stated that *P. aeruginosa* has been isolated from 4% to 20% of patients experiencing acute COPD. This condition results from the colonization of *P. aeruginosa* due to prolonged hospitalization and long-term prognosis in patients.[1,3] Once the development of colonized *P. aeruginosa* begins, it results in prominent adaptive alterations in chronic airway infections. These infections include resistance to antibiotics, increased synthesis of mucoid

[a]*Quorum Sensing Laboratory, Centre for Research in Infectious Diseases (CRID), School of Chemical and Biotechnology, SASTRA Deemed to be University, Thanjavur, India. E-mail: adlineprinzy@sastra.ac.in*

[b]*Department of Industrial and Engineering Chemistry, Institute of Chemical Technology, Bhubaneswar, Odisha, India*

‡ Equal contribution.

and mutation rate, loss of O antigen, and cell motility.[2] Biofilm formation is one of the key virulence factors responsible for the pathogenesis of *P. aeruginosa*. Biofilms formed by notorious *P. aeruginosa* can be formed on various surfaces, resulting in increased antibiotic resistance and causing persistent infections. The innate and acquired immune defenses are disabled by bacteria and form a biofilm once in the host. Additionally, they have the potential to produce virulence factors that can cause serious tissue damage. This biofilm formation has the advantage of protecting and shielding bacteria from external stress, including phagocytosis, allowing for long-term colonization and persistence in host cells.[5] This biofilm formation encapsulates *P. aeruginosa*, which is essential for its survival, persistence, and long-term colonization.[6] As a result of the inherent antibiotic resistance and adaptability of *P. aeruginosa*, regular antibiotics fail to function effectively, thereby resulting in higher mortality rates. Owing to the inherent antibiotic resistance and adaptability of *P. aeruginosa*, regular antibiotics fail to work against it, resulting in higher mortality rates.[7] Ensifentrine (ENF) is an FDA-approved drug with anti-inflammatory properties against COPD and is a dual inhibitor of phosphodiesterases 3 and 4.[8] In June 2024, the drug was approved under the trade name Ohtuvayre. Existing FDA-approved phosphodiesterase (PDE) inhibitors are selective against either PDE3 or PDE4, and ENF exhibits an outstanding clinical profile. It possesses excellent tolerability, effectiveness, and safety by inhibiting both PDE3 and PDE4.[9] Airway hyper-responsiveness is a prominent feature related to exacerbations of COPD, which are reduced by the action of ENF.[8] PDEs regulate the functioning of the airway smooth muscle tone and inflammation by regulating cyclic nucleotides. Because ENF is a dual inhibitor of PDE3 and PDE4, it exhibits an additive or synergistic phenomenon.[10] The mechanism of action that ENF adapts is to elevate the levels of intracellular cyclic adenosine monophosphate (cAMP), which leads to reduced inflammation and enhanced mucociliary clearance.[9]

Biofilms are associated with more than 80% of chronic bacterial infections, and there is a high need to combat biofilm-related infections.[11] The overuse of antibiotics causes the emergence of resistant strains, and alternative strategies are required to prevent the biofilm formation of *P. aeruginosa*. Hence, the development of novel antibiotics, quorum sensing (QS) inhibitors, bacteriophages, and anti-biofilm agents is underway.[12] However, these strategies possess several challenges, including high costs, regulatory hurdles and the potential for resistance development. Drug repurposing focuses on identifying a new therapeutic application for an existing drug, which is believed to be cost-effective and solves these obstacles.[13] Although ENF has been shown to enhance the function of the lung and the quality of life in COPD patients, its potential anti-pathogenic effects, particularly against *P. aeruginosa*, remain underexplored. To bridge this gap, our study focuses on a novel synthetic route for ENF that involves the synthesis of multiple intermediates. This will help improve the yield and purity of the final product. More importantly, we tested these intermediates for their individual anti-pathogenic properties, providing insight into the roles they might play in

the overall efficacy of ENF. By leveraging the safety profiles and established pharmacokinetics of approved drugs, repurposing offers a faster transition from bench to bedside than *de novo* drug development. The rationale for investigating ENF concerning biofilm inhibition stems from emerging evidence that PDE inhibitors can influence bacterial signaling pathways and biofilm dynamics.[14] Specifically, in this study, we hypothesize that ENF and its intermediates may interfere with the key pathways involved in the formation of biofilms in *P. aeruginosa*, thereby reducing its pathogenicity.

Results and discussion

Synthesis and characterization

Synthesis begins with the reaction of 2-(3,4-dimethoxyphenyl) ethanamine and urea under acidic conditions to produce 1-(3,4-dimethoxyphenethyl) urea (ENF^U). This compound then reacts with diethyl malonate in the presence of sodium ethoxide and ethanol to form 1-(3,4-dimethoxyphenyl) barbituric acid (ENF-barbituric acid). Next, ENF-barbituric acid is chlorinated using phosphorus oxychloride, yielding 2-chloro-9,10-dimethoxy-6,7-dihydro-4*H*-pyrimido[6,1-*a*]isoquinolin-4-one (ENF^C). The ENF^C intermediate subsequently undergoes a substitution reaction with 2,4,6-trimethylaniline (2,4,6-TMA), resulting in the formation of 9,10-dimethoxy-2-(2,4,6-trimethylphenylimino)-3,4,6,7-tetrahydro-2*H*-pyrimido[6,1-*a*]isoquinolin-4-one (ENF^T). Subsequently, ENF^T reacts with 2-(2-bromoethyl) phthalimide to produce 9,10-dimethoxy-2-(2,4,6-trimethylphenylimino)-3-(2-*N*-phthalimidoethyl)-3,4,6,7-tetrahydro-2*H*-pyrimido[6,1-*a*] isoquinolin-4-one (ENF^P). The ENF^P intermediate was then treated with hydrazine hydrate, resulting in the formation of 9,10-dimethoxy-2-(2,4,6-trimethylphenylimino)-3-(2-amino-ethyl)-3,4,6,7-tetrahydro-2*H*-pyrimido[6,1-*a*]isoquinolin-4-one (ENF^A). Finally, ENF^A is converted to the finished ENF drug in the presence of sodium cyanide and water. All the above intermediates (ENF^U, ENF-barbituric acid, ENF^C, ENF^T, ENF^P, and ENF^A) and the drug ENF were confirmed through ^{1}H, ^{13}C NMR, HRMS and IR data.

Antibacterial activity

The rise of AMR in bacterial strains emphasizes the limitations of single-targeted drugs. Novel alternative therapeutic measures must be taken to tackle this silent pandemic, AMR.[15] To overcome this issue, our study relied on an understanding of the bifunctional effect of ENF as a bronchodilator and an anti-biofilm agent. There are no published data currently available that report on the antimicrobial activity of ENF. Our current study demonstrates the antimicrobial activity of ENF and its intermediates. The results of this study provide critical insights into the antibacterial activity of the compound, showing that ENF and its intermediates (ENF^A, ENF^U, ENF^T, ENF^P, and ENF^C) do not exhibit any significant growth inhibition effect against the tested strain across varying concentrations ranging from 500 μM to 0.25 μM. The figure in the ESI† shows the dose-dependent graphs for all the compounds with varying concentrations against the percentage of inhibition. As these

compounds did not show growth inhibition effects, we evaluated the potential of all these compounds in retarding the biofilm formation (Fig. 1).

Antibiofilm activity and visualization

The colonization of bacteria and the formation of biofilms play a crucial role in evading the host immune response. The development of biofilms in the COPD patient's lungs even worsens the condition. *P. aeruginosa* is known for its ability to form biofilms and complex microbial communities embedded in a self-produced extracellular polymeric substance (EPS) matrix, contributing to its antibiotic resistance and persistence in the host.[16] The biofilm inhibition ability of the compounds was determined by employing a CV assay. A significant dose-dependent biofilm inhibition of 50–60% was observed in ENF and ENF[A] across varying concentrations ranging from 7.9 to 0.9 µM. Our results indicate that ENF and its intermediates did not significantly inhibit growth at different concentrations, but they showed considerable anti-biofilm activity, especially for ENF and ENF[A]. The other intermediates (ENF[U], ENF[T], ENF[P], and ENF[C]) do not exhibit any significant biofilm inhibition across the same concentration. These findings align with the growing literature, indicating that biofilm inhibition can occur without directly impacting bacterial growth in planktonic culture.[17] The two potent compounds ENF and ENF[A] were chosen with their lowest biofilm inhibition concentrations for further experiments. Fig. 2 is a combined graph of the MIC and MBIC of the compounds ENF and ENF[A] at varying concentrations ranging from 500 µM to 0.25 µM.
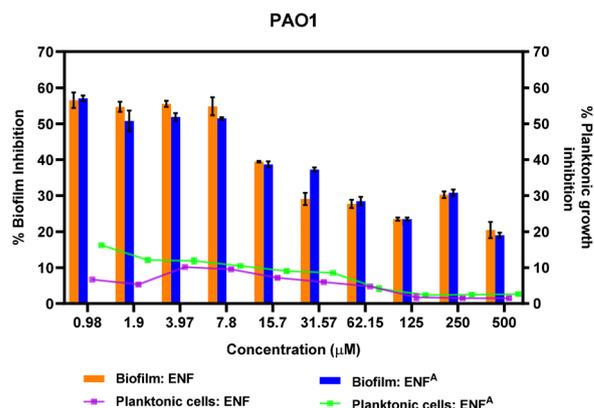

Fig. 2 Determination of the minimum inhibitory concentration and minimum biofilm inhibitory concentration of ENF and ENF[A] at varying concentrations against PAO1.

The qualitative analysis results substantiated the data obtained from the quantitative analysis of biofilm inhibition. Significant biofilm retardation was observed through the CV staining of the compounds ENF and ENF[A] across varying concentrations ranging from 7.9 µM to 0.9 µM (Fig. 3). A dense network of biofilm was observed in the control, and upon treatment with the respective compound, the development of biofilm was inhibited significantly. The remaining intermediates did not show significant biofilm inhibition, indicating the specificity of the anti-biofilm activity of ENF and ENF[A]. The biofilm inhibition observed suggests that these compounds interfere with the early stages of biofilm formation rather than
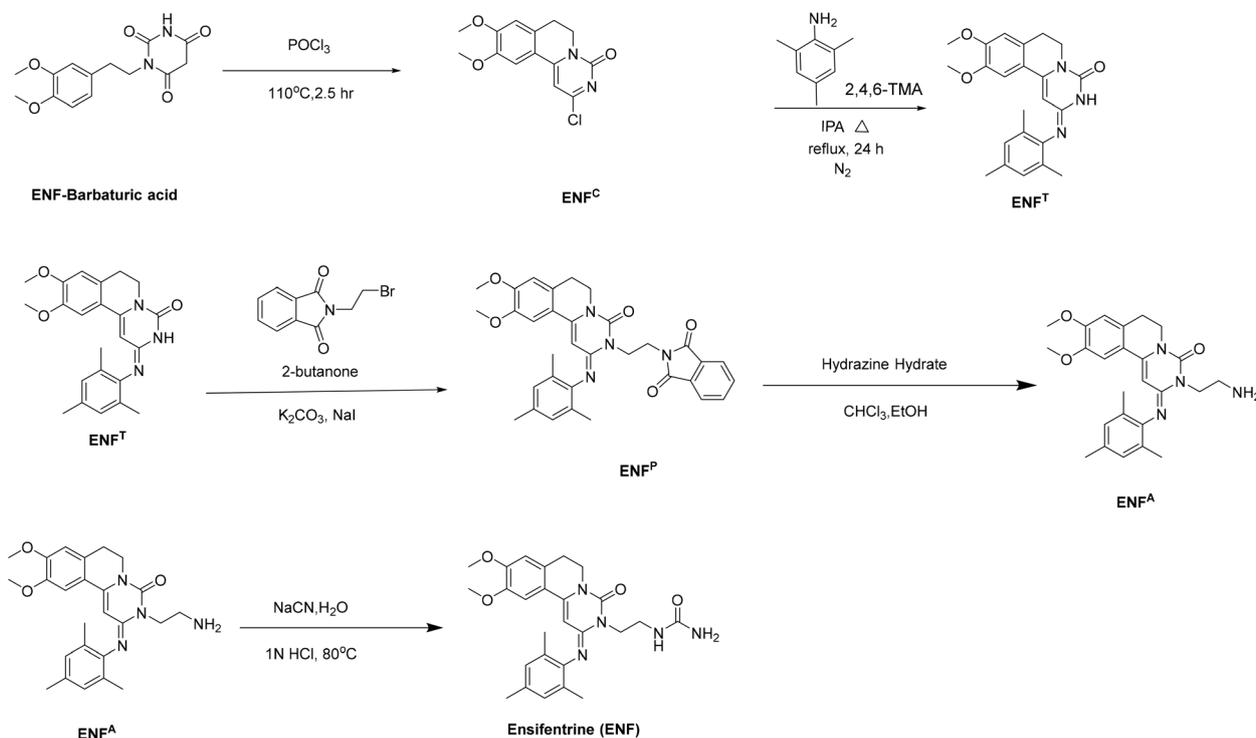

Fig. 1 Synthesis of ENF and its intermediates (ENF[A], ENF[B], ENF[U], ENF[T], ENF[P], and ENF[C]).
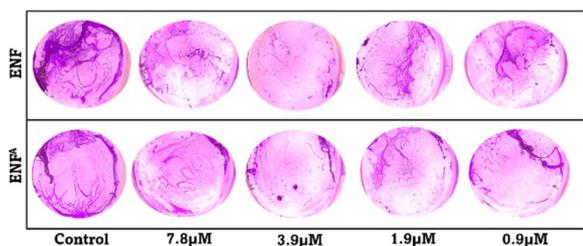
Fig. 3 Qualitative analysis of biofilm inhibition at varying concentrations of ENF and ENF[A] performed using the crystal violet assay and visualized under a stereomicroscope.

simply disrupting pre-existing biofilms, as confirmed by biofilm visualization under a stereo microscope. This finding aligns with those of previous studies, showing that biofilm inhibition can occur *via* the disruption of bacterial adhesion or extracellular matrix production. *P. aeruginosa* biofilms developed within the lung cavities of patients suffering from COPD are prone to exacerbate the disease process and result in worse clinical outcomes due to increased resistance to both host immunity and conventional antibiotics.[18]

Effect on pyoverdine production

Biofilm formation is largely facilitated by the production of EPS and virulence factors, such as PVD, a siderophore critical for iron acquisition and biofilm maturation. PVD is a low-molecular-weight siderophore involved in the QS regulating pathways of *P. aeruginosa*. This PVD complex enhances *P. aeruginosa* virulence not only by facilitating iron uptake but also by triggering inflammation and oxidative damage in the host through its redox-cycling activity.[19,20] The production of PVD upon treatment was quantified for the compounds ENF and ENF[A] across various concentrations ranging from 3.9 to 0.9 μM. A significant reduction of 30–35% was observed in the treatment of ENF, and a 40–45% reduction was observed after the treatment with ENF[A], as shown in Fig. 4. This shows that PVD could be a target of ENF in inhibiting biofilm formation. This leads to inflammation in the host during chronic *Pseudomonas*

infections in COPD patients. Numerous studies have been carried out, and recent approaches to fighting *P. aeruginosa* have focused on exploiting its iron homeostasis mechanisms, turning its greatest strength into a provable weakness.[21–24] Moreover, there was a reduction in PVD production after ENF and ENF[A] treatment, with ENF[A] causing a slightly higher reduction in PVD (45% compared to 35% for ENF). As PVD is implicated in the QS pathways of *P. aeruginosa*, it implies that ENF and ENF[A] may control the *P. aeruginosa* QS pathway, which is highly renowned for its mechanism of biofilm development and maintenance. The inhibition of PVD synthesis can thus be taken as an indirect QS inhibitor marker that further contributes to the effectiveness of these compounds in anti-biofilm activity.[25]

Effect on the EPS production

Capitalizing on the encouraging outcomes of the PVD quantification assay, the test compounds ENF and ENF[A] were also examined owing to their ability to lower EPS production by PAO1. The matrix of the EPS comprises polysaccharides, proteins, and extracellular DNA. This protects the bacterial cells against environmental stress and prevents antimicrobial penetration. Further studies are needed to understand the exact mechanism by which ENF and its intermediate prevent biofilm formation. At the tested concentration (from 7.9 μM to 1.9 μM), ENF and ENF[A] resulted in a significant reduction in EPS production, achieving a 35–40% decrease compared to the control. The highest amount of EPS inhibition was observed at 1.9 μM. Early findings suggest that the compounds can disrupt the QS pathways of *P. aeruginosa*, such pathways being critical for biofilm development. *P. aeruginosa* needs QS to control the production of EPS, which forms the structural matrix of biofilms. Disruption of QS signaling can lower EPS production and compromise the integrity of the biofilm, rendering healthy bacterial cells more vulnerable to antimicrobial therapies.[26] Our findings indicate that the ENF and its intermediate ENF[A] may be modulators of the QS system, and this needs to be verified through additional molecular gene expression analysis (Fig. 5).
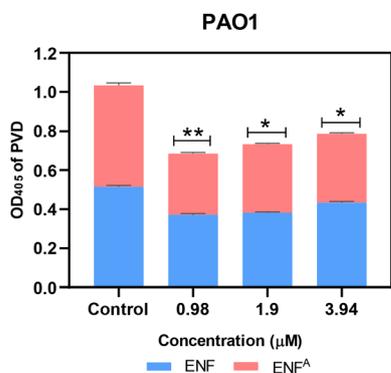

Fig. 4 OD value of the PAO1 cell suspension and its supernatant containing pyoverdine measured at 405 nm using a spectrophotometer ($n = 3$, ***$p < 0.0001$, ****$p < 0.0001$ compared with the control).
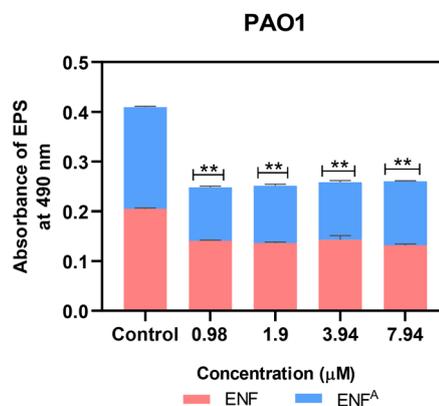

Fig. 5 Quantification of EPS in PAO1 treated with ENF and ENF[A] at its varying biofilm inhibitory concentration ($n = 3$, ***$p < 0.0001$, ****$p < 0.0001$ compared with the control).

Checkerboard assay

This suggests that there is an urgent requirement for alternative approaches that need to enhance the efficacy of the available antibiotics. This study assessed the combinatory potential of ENF with ciprofloxacin (CIP) using a checkerboard assay; then, the results were subjected to the Bliss independence model. According to this model, a Bliss score greater than 0 indicates synergy, a score less than 0 denotes antagonism, and a score of 0 reflects an additive effect. It was observed that there was a synergistic interaction between ENF and CIP at certain concentrations, suggesting the potential of ENF to enhance the antimicrobial activity of CIP against *P. aeruginosa*. This combination was the most effective. Fig. 7 shows 65–70% inhibition when ENF was used at a concentration of 3.9 μM in the presence of 0.25 μg per mL CIP. The Bliss score at this combination was 54.13, which is considered to be quite a significant synergy given that it complements the action of CIP and enhances its bactericidal effect at lower concentrations. Apart from CIP, the combinatorial activity of ENF was tested with several antibiotics, such as doxycycline, ceftazidime, amoxicillin and carbapenem. However, they did not show any significant synergistic activity when combined with ENF. This combinatory effect is particularly useful in reducing the dose of antibiotics needed, thereby reducing the associated side effects and slowing the development of resistance in pathogenic bacteria. The underlying mechanism of this synergy may be related to the disruption of the biofilm structure by ENF, which enhances the penetration and efficacy of CIP. Biofilms act as protective barriers that limit the diffusion of antibiotics, reducing their potency. ENF's antibiofilm activity likely contributes to the observed enhancement of CIP's effectiveness. In addition, the interaction between ENF and CIP might affect bacterial metabolic pathways, further potentiating their combined antimicrobial action. Interestingly, although ENF clearly demonstrated synergy with CIP, its intermediate compound, ENF^A, did not. This distinction indicates that the particular structural features of ENF are important for its synergy with CIP. Further structural and mechanistic studies are required to clarify these differences and optimize the combinatory potential of ENF derivatives. Thus, an adjuvant role of ENF may be observed in enhancing CIP's activity, offering an innovative approach toward combating biofilm-associated infections. This finding is consistent with earlier studies that highlight the benefits of using biofilm-disrupting agents in combination with antibiotics that counteract the protective barrier developed by biofilms (Fig. 6).

Effect on biofilm eradication

The ability of *P. aeruginosa* to form robust pre-formed biofilms challenges the management of lung infections, especially in COPD patients. Biofilms are notoriously resistant to conventional therapies, reducing the efficiency of drugs and contributing to persistent infections. This study aims to investigate the potential of ENF and its intermediate, ENF^A, to eradicate biofilms at their respective biofilm inhibitory concentrations (from 7.9 μM to 1.9 μM). A well-defined biofilm network was observed

with fluorescence microscopy and live–dead staining in the control, which indicated the resilience and structural complexity of *P. aeruginosa* biofilms. Although the degree of biofilm reduction varied among the different concentrations, eradication was observed at all tested concentrations compared to the control. However, there was a maximum reduction in biofilm formation after treatment with ENF and ENF^A, significantly at a concentration of 7.9 μM. This result shows that ENF and ENF^A possess dose-dependent antibiofilm activity, where higher concentrations result in a more significant effect. More importantly, as depicted in Fig. 7, the fluorescence microscopy results correlate with the quantitative data obtained from the biofilm inhibition assays, thus enhancing the validity of our observations. The dual action of disruption of the biofilm structure and the killing of bacteria can explain the efficacy of ENF and ENF^A. The penetration of live cells by acridine orange (AO) and the staining of dead cells by propidium iodide (PI) with well-defined visual feedback of biofilm eradication established fluorescence microscopy as an excellent tool for assessing antibiofilm activity. The decreased biomass of biofilm formation explains the ability of these compounds to penetrate beyond the protective barriers of a biofilm, making them more effective therapeutics. These results confirm the potential of ENF and its derivatives as antibiofilm agents in the fight against *P. aeruginosa*. Nevertheless, more studies need to be carried out to understand the exact molecular mechanisms behind their actions and to evaluate them *in vivo*. This work advances the literature by finding new approaches to treat biofilm-related infections, especially targeting vulnerable populations, such as those with COPD.

Experimental

Synthesis and characterization

ENF^U (intermediate) and 1-(3,4-dimethoxyphenyl) barbituric acid (ENF-barbituric acid) were synthesized from the reported procedures.

For ENF^U

White powder. ^{1}H NMR (400 MHz, CDCl$_3$) δ 6.80 (d, J = 7.9 Hz, 1H), 6.75–6.71 (m, 2H), 4.74 (s, 1H), 4.43 (s, 2H), 3.85 (d, J = 3.8 Hz, 6H), 3.41 (dd, J = 12.8, 6.7 Hz, 2H), 2.76 (t, J = 6.8 Hz, 2H).

^{13}C NMR (101 MHz, CDCl$_3$) δ 158.60 (s), 149.02 (s), 147.66 (s), 131.55 (s), 120.73 (s), 112.07 (s), 111.43 (s), 55.92 (d, J = 4.9 Hz), 41.83 (s), 35.74 (s).

IR (UATR) ν_{max}: N–H (3446, 3335), C=O (1646), C–N (1256), and C–O (1231) cm^{-1}

HRMS (ESI) calcd for C$_{11}$H$_{16}$N$_2$O$_3$ [M + Na]$^+$ 247.1070; found 247.1059.

For ENF-barbituric acid

Beige powder. ^{1}H NMR (400 MHz, CDCl$_3$) δ 8.23 (s, 1H), 6.75–6.69 (m, 3H), 4.00 (dt, J = 14.5, 6.2 Hz, 2H), 3.80 (d, J = 10.2 Hz, 6H), 3.54 (s, 2H), 2.82–2.76 (m, 2H).

^{13}C NMR (101 MHz, CDCl$_3$) δ 164.93 (s), 164.09 (s), 150.11 (s), 149.02 (s), 147.93 (s), 130.04 (s), 120.96 (s), 112.12 (s), 111.30 (s), 55.93 (d, J = 1.9 Hz), 42.56 (s), 39.25 (s), and 33.53 (s).
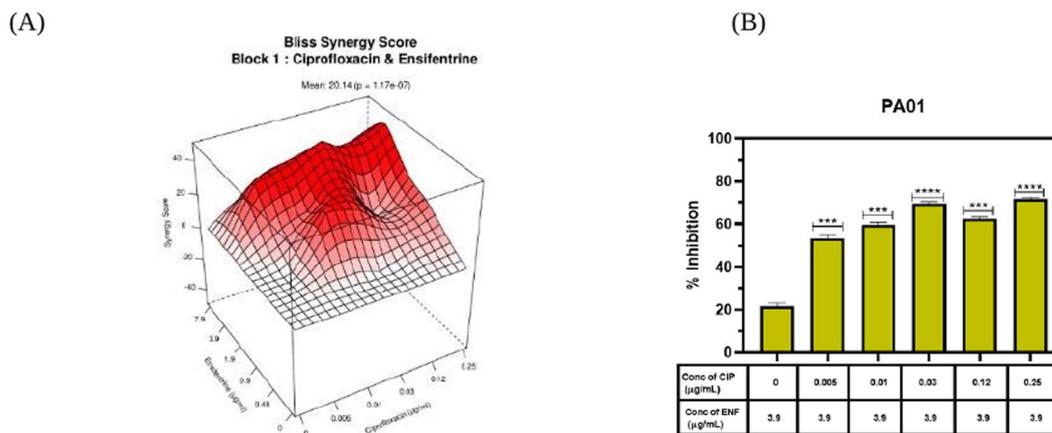
(A)

Bliss Synergy Score
Block 1 : Ciprofloxacin & Ensifentrine

Mean: 20.14 (p = 1.17e-07)

(B)

Fig. 6 Effect of ENF in enhancing the bactericidal activity of CIP. (A) Synergy plot illustrating the combined effect of ENF and CIP at varying concentrations against PAO1. (B) Potentiation of CIP was observed at a minimum concentration of 0.25 μg mL^{-1}, with ENF maintained at a constant concentration of 3.9 μM for PAO1 ($n = 3$, ***$p < 0.0001$, ****$p < 0.0001$ compared with the control).

IR (UATR) ν_{max}: nN–H (3385), mC = O (1662), sC–O (1269), sC–N (1207) cm^{-1}.

HRMS (ESI) calcd for $C_{14}H_{16}N_2O_5$ [M + Na]$^+$ 315.0961; found 315.0957.

Step 1 (ENF-barbituric acid to ENF^C).[27–30] 1-(3,4-Dimethoxyphenyl) barbituric acid (IN-II) was refluxed with phosphorus oxychloride for 2.5 h. Upon warming, the excess phosphorous oxychloride was eliminated by distillation (20 mmHg). The residue on cooling was formed into a slurry in dioxane and slowly added to a forcefully shaken ice/water solution. Chloroform was added to the mixture after basification with a 30% sodium hydroxide solution. Before extracting the aqueous phase with chloroform, the organic layer was separated. The organic extracts were combined and washed with water, dried over magnesium sulfate, and concentrated *in vacuo* to give a tacky residue. This was shaken with methanol for a few minutes, filtered and washed with methanol and diethyl ether, and dried *in vacuo* at 40 °C to give the title compound as a yellow/orange solid.

Yellow/orange solid, yield: 62%. ^{1}H NMR (400 MHz, CDCl$_3$) δ 6.73 (s, 2H), 6.04 (s, 1H), 4.10–4.06 (m, 2H), 3.95 (s, 3H), 3.92 (s, 3H), 2.95 (t, $J = 6.3$ Hz, 2H).

^{13}C NMR (101 MHz, CDCl$_3$) δ 163.62 (s), 152.14 (s), 151.72 (s), 149.18 (s), 148.56 (s), 130.72 (s), 119.24 (s), 111.40 (s), 109.53 (s), 95.65 (s), 56.40 (s), 56.24 (s), and 27.26 (s).

IR (UATR) ν_{max}: C=N (1664), C=O (1641), C–N (1260), C–O (1153) cm^{-1}.

HRMS (ESI) calcd for $C_{14}H_{13}ClN_2O_3$ [M + Na]$^+$ 315.7245; found 315.0633.

Step 2 (ENF^C to ENF^T).[29–32] 2-Chloro-9,10-dimethoxy-6,7-dihydro-4*H*-pyrimido[6,1-*a*]isoquinolin-4-one (IN-III), which was prepared, was stirred and refluxed in propan-2-ol with 2,4,6-trimethylaniline under a nitrogen atmosphere for 24 h. The solution was cooled to room temperature and evaporated *in vacuo*, and the residue was then purified by column chromatography on silica gel using CH$_2$Cl$_2$/MeOH as the eluent,

initially 98 : 2, which was altered to 96 : 4 once the product started to elute from the column.

Yellow solid, yield: 67%. ^{1}H NMR (400 MHz, CDCl$_3$) δ 11.62 (s, 1H), 6.92 (d, $J = 6.6$ Hz, 2H), 6.74 (s, 1H), 6.68 (s, 1H), 5.44 (s, 1H), 4.11 (t, $J = 6.5$ Hz, 2H), 3.89 (s, 3H), 3.72 (s, 3H), 2.98 (t, $J = 6.5$ Hz, 2H), 2.26 (s, 3H), 2.21 (s, 6H).

^{13}C NMR (101 MHz, CDCl$_3$) δ 157.27 (s), 154.66 (s), 154.37 (s), 148.95 (s), 146.91 (s), 139.15 (s), 135.33 (s), 132.29 (s), 129.67 (s), 129.06 (s), 117.45 (s), 110.96 (s), 109.70 (s), 83.50 (s), 56.71 (s), 40.34 (s), 21.06 (s), 18.25 (d, $J = 11.4$ Hz).

IR (UATR) ν_{max}: N–H (3347), C=N (1688), C=O (1635), C–N (1271), and C–O (1217) cm^{-1}.

HRMS (ESI) calcd for $C_{23}H_{26}N_3O_3$ [M + H]$^+$ 392.2007; found 392.1974.

Step 3 (ENF^T to ENF^P).[29–32] A solution of (IN-IV), potassium carbonate, sodium iodide and *N*-(2-bromoethyl)phthalimide in 2-butanone was heated under reflux with stirring under nitrogen for 4 days. The mixture was cooled to room temperature, and the filtrate was evaporated under a vacuum. The residue was treated with methanol, and the solid was filtered off, washed with methanol and recrystallized from ethyl acetate to produce the compound as a pale yellow solid. Evaporation of the mother liquor and column chromatography of the residue over silica gel (CH$_2$Cl$_2$/MeOH 95 : 5) gave the final product.

Pale yellow solid, yield: 46%. ^{1}H NMR (400 MHz, CDCl$_3$) δ 7.81 (dd, $J = 5.4, 3.0$ Hz, 2H), 7.72–7.64 (m, 2H), 6.85 (s, 2H), 6.73 (s, 1H), 6.61 (s, 1H), 5.47 (s, 1H), 4.65–4.59 (m, 2H), 4.26–4.21 (m, 2H), 3.88 (s, 3H), 3.79 (d, $J = 6.0$ Hz, 2H), 3.76 (s, 3H), 2.77 (t, $J = 6.1$ Hz, 2H), 2.26 (s, 3H), 2.06 (s, 6H).

^{13}C NMR (101 MHz, CDCl$_3$) δ 168.64 (s), 152.11 (s), 151.63 (s), 148.53 (s), 148.29 (s), 144.07 (s), 142.14 (s), 133.67 (s), 132.42 (s), 129.82 (s), 128.55 (d, $J = 8.6$ Hz), 120.03 (s), 110.42 (s), 108.83 (s), 89.24 (s), 56.47 (s), 56.02 (s), 40.85 (s), 40.11 (s), 25.37 (s), 20.75 (s), 18.29 (s).

IR (UATR) ν_{max}: C=O (1774, 1725 (phthalimide), (1640), C=N (1688), C–N (1385, C–O (1210) cm^{-1}.
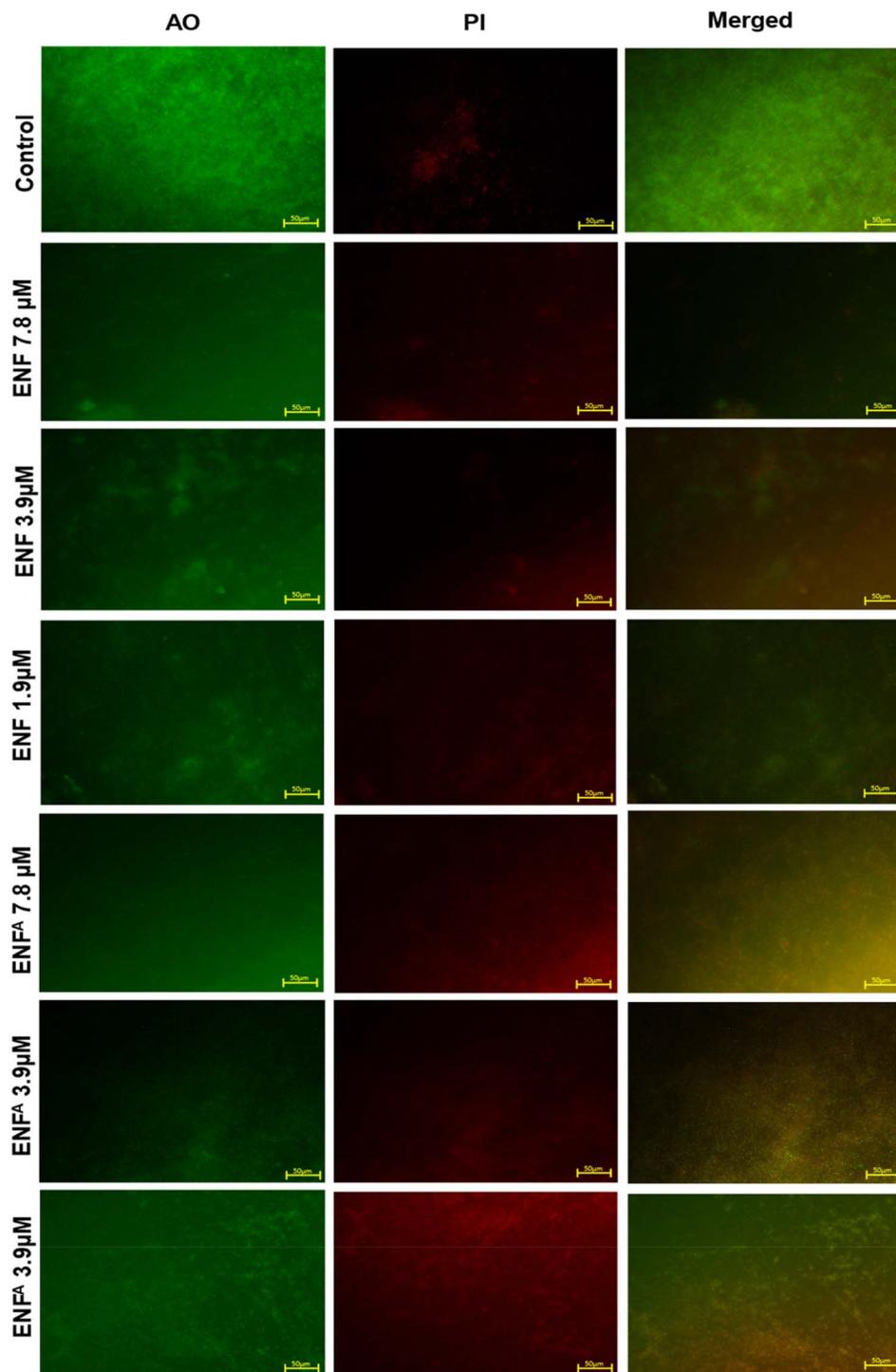
Fig. 7 Merged fluorescence images of the PAO1 biofilm stained with AO/PI, depicting live cells in green and dead cells in red after treatment with different biofilm eradication concentrations, with the untreated control.

HRMS (ESI) calcd for $C_{33}H_{32}N_4O_5$ $[M + H]^+$ 565.6401; found 565.2452.

Step 4 (ENF^P to ENF^A).[29–32] A solution of 9,10-dimethoxy-2-(2,4,6-trimethylphenylimino)-3-(2-N-phthalimidoethyl)-3,4,6,7-tetrahydro-2H-pyrimido[6,1-a]isoquinolin-4-one and hydrazine hydrate in chloroform and ethanol was stirred at room temperature under nitrogen for 18 h. Additional hydrazine hydrate was added, and the mixture was stirred for a further 4 h. After ice/water cooling, the solid was filtered off, and the filtrate was evaporated *in vacuo*. The residue was dissolved in dichloromethane, and the insoluble material was filtered off. The filtrate was dried over $MgSO_4$ and evaporated under vacuum to give the title compound as a yellow foam.

Yellow foam, 96%. ^{1}H NMR (400 MHz, CDCl$_3$) δ 7.85 (dd, $J =$ 5.4, 3.1 Hz, 1H), 7.71 (dd, $J =$ 5.4, 3.1 Hz, 1H), 6.91 (s, 2H), 6.68 (s, 1H), 6.65 (s, 1H), 5.51 (s, 1H), 4.15 (t, $J =$ 6.0 Hz, 2H), 3.90 (s, 3H), 3.73 (s, 3H), 3.19 (s, 2H), 2.98 (t, $J =$ 6.0 Hz, 2H), 2.28 (s, 3H), 2.18 (s, 6H).

IR (UATR) ν_{max}: N–H (3380), C=N (1697), C=O (1623), C–N (amide, 1262), C–O (1210) cm^{-1}.

HRMS (ESI) calcd for C$_{25}$H$_{30}$N$_4$O$_3$ [M + H]$^+$ 435.5413; found 435.2304.

Step 5 (ENF^A to ENF).[29-32] A dropwise addition of a water solution of sodium cyanate was made into a stirred solution of 9,10-dimethoxy-2-(2,4,6-trimethylphenylimino)-3-(2-amino-ethyl)-3,4,6,7-tetrahydro-2H-pyrimido[6,1-a]isoquinolin-4-one. The aforesaid solution was a stirred solution of mixing water and 1 N HCl at 80 °C and stirred for 2 h. The ice-bath-cooled mixture was basified with 2 N NaOH. Extraction with dichloromethane was followed by drying with magnesium sulphate and *in vacuo* evaporation. The yellow foam obtained was column chromatographed on silica gel using CH$_2$Cl/MeOH (97 : 3) as the eluent and triturated with ether to give the title compound a yellow solid.

Yellow solid, yield: 54%. ^{1}H NMR (400 MHz, DMSO-d$_6$) δ ppm: 6.97 (s, 1H), 6.86 (s, 2H), 6.67 (s, 1H), 6.11 (t, $J =$ 5.8 Hz, 1H), 5.46 (s, 2H), 5.33 (s, 1H), 4.19 (t, $J =$ 6.8 Hz, 2H), 3.92 (t, $J =$ 6.0 Hz, 2H), 3.81 (s, 3H), 3.62 (s, 3H), 3.18 (d, $J =$ 5.2 Hz, 1H), 2.91 (t, $J =$ 5.9 Hz, 2H), 2.23 (s, 3H), 1.98 (s, 6H).

^{13}C NMR (101 MHz, DMSO-d$_6$) δ ppm: 159.10, 152.19, 151.45, 148.64, 148.29, 144.53, 142.78, 131.07, 130.77, 128.86, 128.20, 119.36, 111.84, 109.05, 88.17, 56.55, 56.20, 41.97, 37.36, 27.50, 20.91, and 18.49.

IR (UATR) ν_{max}: N–H (3386), C=N (1660), C=O (1647), C–N (1270), C–O (1206) cm^{-1}.

HRMS (ESI) calcd for C$_{26}$H$_{31}$N$_5$O$_4$ [M + H]$^+$ 478.5733; found 478.2401.

Evaluation of the anti-pathogenic effects

Pathogen preparation and culture conditions. The PAO1 strain of *P. aeruginosa* was employed as the model bacterial strain for the experimental investigations. The overnight culture was prepared by transferring aliquots (10 μL) of culture from the glycerol stock to the tubes containing 2 mL of Tryptic soya broth (TSB) and incubated at 37 °C for 18–24 hours. After incubating for 24 hours, the overnight culture was centrifuged at 6000 rpm for 10 min and resuspended in fresh TSB broth. The resuspension was swabbed onto Tryptic Soya Agar (TSA) and incubated for 18–24 h at 37 °C. The plates were stored at 4 °C for future use. All the required chemical reagents and media were purchased from Hi Media, Mumbai.

Antibacterial assay. The minimum inhibitory concentration values for ENF and its intermediates ENF^A, ENF^U, ENF^T, ENF^P, and ENF^C were determined by broth microdilution assay. When the fresh colonies of the PAO1 strain were grown in TSB broth, the culture was maintained at 37 °C for 18–24 hours. Each compound was prepared in DMSO solvent to give a stock solution of 30 mg mL^{-1}. Then, 100 μL of the stock solution was serially diluted two-fold in TSB media in 96-well microplates to give a final concentration of 500–0.25 μM for each compound. The overnight bacterial culture was diluted to 1 : 100 in fresh TSB. 10 μL of the bacterial suspension was added to the wells containing the diluted compounds. The microplate was then incubated at 37 °C for 18–24 h. The optical density was measured at 595 nm (OD$_{595}$) using BioRadi-Mark after incubation. MIC was defined as the minimal concentration of the compound exhibiting no visible growth of the organisms. The microdilution assay was performed in triplicate for reliable results.[33]

Antibiofilm assay. The biofilm inhibition ability of ENF and its intermediates was tested against strain PAO1 using a crystal violet assay. According to the MIC protocol, the PAO1 overnight culture was diluted and then added to a 96-well plate containing serial dilutions of ENF and its intermediates (from 500 μM to 0.9 μM). The TSB medium supplemented with 0.2% glucose was used as the culture medium. The optical density at OD$_{595}$ of the planktonic cells was determined after incubation at 37 °C for 24 h. The plate was then lightly tapped to remove non-adherent planktonic cells, washed twice with 1% PBS, and allowed to air-dry for 5–10 minutes. Then, the cells were stained with 150 μL of 0.2% crystal violet for 15–20 minutes. Following incubation, the surplus stain was removed by washing with water, and the stain bound to the biofilm was eluted with 200 μL of 33% acetic acid. The OD was measured at 595 nm.[34] This procedure was performed in triplicate to obtain reliable results.

Crystal violet staining. Crystal violet staining was used to visually evaluate the inhibitory ability of ENF and ENF^A in biofilm formation. The overnight culture of PAO1 was diluted at a 1 : 100 ratio. The culture was plated in a 24-well plate containing 1 mL of TSB supplemented with 0.2% glucose. The plate was treated with different biofilm inhibitory concentrations (ranging from 7.9 μM to 0.9 μM) of ENF and ENF^A. Wells without any treatment served as the control. After incubation for 24 h at 37 °C, unattached planktonic cells were carefully aspirated and the wells were washed twice with PBS and air-dried for 5–10 minutes. Then, 500 μL of 0.2% CV was added and incubated for 15–20 min to stain the cells. Excessive staining was removed by rinsing with deionized water, and the plate was allowed to dry in the air. Stereo microscopy (IVESTA3 Stereomicroscope) was employed to observe the biofilm retardation on the 24-well plate.

Exopolysaccharide assay. The compounds that showed significant biofilm retardation were chosen for further assays (ENF and ENF^A). PAO1 cells were grown in a 24-well microtiter plate containing 1 mL of TSB and 0.2% glucose to induce biofilm formation. The wells were treated with and without ENF and ENF^A at concentrations ranging from 7.9 μM to 0.9 μM using a modified protocol described in a previous study,[35] and the plate was incubated for 24 h at 37 °C. EPS was quantified by a total carbohydrate assay. After 24 h of incubation, the wells were washed with 1× PBS (0.5 mL) and treated with an equal volume of 5% phenol along with five volumes of concentrated H$_2$SO$_4$. The culture plate was incubated in the dark for 1 h, and the absorbance was recorded at OD$_{490}$ using a Thermo Scientific Evolution 201 UV-vis spectrophotometer.

Pyoverdine assay. A fresh casamino acid medium was inoculated with a 1 : 100 dilution of an overnight culture of PAO1

using modifications based on the protocol described by.[15] TSB was used as the culture medium, and biofilm inhibitory concentrations of ENF and ENF^A ranging from 3.9 μM to 0.9 μM were given as treatment. After incubation for 24 h at 37 °C, the pyoverdine (PVD) from the culture was extracted by centrifugation, and the absorbance of the supernatants was measured at 405 nm using a Thermo Scientific Evolution 201 UV-vis spectrophotometer.

Checkerboard assay. The ENF-CIP synergistic activity was confirmed by the checkerboard assay. Briefly, ENF was serially double diluted in wells containing 100 μL of TSB starting at their biofilm inhibitory dose of 7.9 μM to 0.9 μM. The CIP doses in the wells varied from 0.25 to 0.001 μg mL^{-1}. Individual concentrations of both compounds were also tested separately as controls. Following the MIC assay protocol, an overnight culture of PAO1 was diluted to a 1:100 ratio and added to 96-well plates. The well plates were incubated at 37 °C for 24 h, and the optical density was measured at 595 nm to determine the percentage of growth inhibition. SynergyFinder Plus was used to evaluate the data obtained using the Bliss independence model, which predicts the combined effect as the product of the individual effects, expressed by the formula $E_i = E_A \times E_B$ output.[36]

Biofilm eradication assay. Fluorescence microscopy imaging was used to evaluate the biofilm eradication ability of ENF and ENF^A using the dilution method. Briefly, the overnight culture of PAO1 was prepared and diluted to 1:100 by following a modification of the procedure described by Kim et al.[34] 200 μL of the inoculum was added to a six-well plate containing 2 mL of TSB prepared with 0.2% glucose. Sterile coverslips were placed in all the wells. The spent culture medium was replaced with fresh TSB every 24 h, and the cultures were incubated at 37 °C under static conditions to allow biofilm development for 48 h. After the respective incubation, the pre-formed biofilms were treated with biofilm inhibitory concentrations of ENF and ENF^A (ranging from 7.9 μM to 1.9 μM) for 24 hours at 37 °C. Wells without treatment served as controls. Following the treatment, the planktonic cells were removed by aspiration, and the coverslips over the wells were washed twice with 1× PBS to ensure that only adherent biofilms remained. Biofilms that adhered to the coverslips were stained using 2 μg mL^{-1} of AO and PI dyes. The stained coverslips were kept in the dark for 10 min. The surplus stain was aspirated and rinsed with 1× PBS. Then, the coverslips were mounted onto sterile glass slides, and the fluorescence images were acquired at 40× magnification using a Nikon Eclipse Ts2 microscope.

Statistical analysis. Statistical analysis was carried out using GraphPad Prism software version 8.0.2 (GraphPad Software Inc., San Diego, CA, USA). The level of statistical significance was assessed using Student's t-test with a cutoff $p \leq 0.05$. The findings were presented as averages along with the standard deviation.

Conclusion

In summary, the results of this study hold promise because the compounds ENF and ENF^A effectively act as antibiofilm agents in the inhibition of biofilm development in *P. aeruginosa*. Its interference in the QS and surface adhesion steps during biofilm formation may provide a great therapeutic opportunity to combat chronic bacterial infections. Further studies must be conducted to elucidate the mechanisms of action and optimize the pharmacological properties of these compounds. ENF, a dual PDE3/PDE4 inhibitor, possesses promising anti-biofilm activity against *P. aeruginosa*. Though mainly applied to respiratory diseases, its capacity to interfere with bacterial signaling could lead to antipathogenic activity against a range of pathogens. Cytotoxicity is low at therapeutic concentrations, but systemic uses need to be considered further. As an adjunct therapy, ENF may augment antibiotic activity by enhancing the penetration of the biofilm and reducing inflammation. However, more *in vivo* pharmacokinetic and toxicity experiments must be conducted to validate its viability for antibacterial use.

Data availability

The datasets generated and analyzed during the current study are available from the corresponding author upon reasonable request.

Author contributions

AS: conceptualization, methodology, and writing – original draft. DJA: methodology and writing – original draft. NP: synthesis. APS: conceptualization, investigation, methodology, supervision, and writing – review & editing. RD: conceptualization, investigation, and writing – review & editing.

Conflicts of interest

The authors declare that they have no conflicts of interest related to this work.

Acknowledgements

References

1 D. Adeloye, P. Song, Y. Zhu, H. Campbell, A. Sheikh, I. Rudan, *et al.*, Global, regional, and national prevalence of, and risk factors for, chronic obstructive pulmonary disease (COPD) in 2019: a systematic review and modelling analysis, *Lancet Respir. Med.*, 2022, **10**(5), 447–458.

2 Y. Xia, *Pseudomonas aeruginosa: Regulation of Pathogenesis and Development of Therapeutic Strategies*, PhD thesis, University of Groningen, 2021, DOI: 10.33612/diss.191399929.

3 J. Eklöf, R. Sørensen, T. S. Ingebrigtsen, P. Sivapalan, I. Achir, J. B. Boel, *et al.*, Pseudomonas aeruginosa and risk of death and exacerbations in patients with chronic obstructive pulmonary disease: an observational cohort study of 22 053 patients, *Clin. Microbiol. Infect.*, 2020, **26**(2), 227–234.

4 E. Gerits, E. Blommaert, A. Lippell, A. J. O'Neill, B. Weytjens, D. De Maeyer, *et al.*, Elucidation of the Mode of Action of a New Antibacterial Compound Active against Staphylococcus aureus and Pseudomonas aeruginosa, *PLoS One*, 2016, **11**(5), e0155139.

5 M. T. T. Thi, D. Wibowo and B. H. A. Rehm, Pseudomonas aeruginosa Biofilms., *Int. J. Mol. Sci.*, 2020, **21**(22), 8671.

6 S. O. Khelissa, M. Abdallah, C. Jama and N. E. Chihib, Actively detached Pseudomonas aeruginosa biofilm cell susceptibility to benzalkonium chloride and associated resistance mechanism, *Arch. Microbiol.*, 2019, **201**(6), 747–755.

7 Q. Lin, J. M. Pilewski and Y. P. Di, Acidic Microenvironment Determines Antibiotic Susceptibility and Biofilm Formation of Pseudomonas aeruginosa, *Front. Microbiol.*, 2021, **12**, 747834.

8 A. Anzueto, I. Z. Barjaktarevic, T. M. Siler, T. Rheault, T. Bengtsson, K. Rickard, *et al.*, Ensifentrine, a Novel Phosphodiesterase 3 and 4 Inhibitor for the Treatment of Chronic Obstructive Pulmonary Disease: Randomized, Double-Blind, Placebo-controlled, Multicenter Phase III Trials (the ENHANCE Trials), *Am. J. Respir. Crit. Care Med.*, 2023, **208**(4), 406–416.

9 J. F. Donohue, T. Rheault, M. MacDonald-Berko, T. Bengtsson and K. Rickard, Ensifentrine as a Novel, Inhaled Treatment for Patients with COPD, *Int. J. Chronic Obstruct. Pulm. Dis.*, 2023, **18**, 1611–1622.

10 D. Singh, F. J. Martinez, H. Watz, T. Bengtsson and B. T. Maurer, A dose-ranging study of the inhaled dual phosphodiesterase 3 and 4 inhibitor ensifentrine in COPD, *Respir Res.*, 2020, **21**(1), 47.

11 H. C. Flemming, J. Wingender, U. Szewzyk, P. Steinberg, S. A. Rice and S. Kjelleberg, Biofilms: an emergent form of bacterial life, *Nat. Rev. Microbiol.*, 2016, **14**(9), 563–575.

12 T. Bjarnsholt, The role of bacterial biofilms in chronic infections, *APMIS, Suppl.*, 2013, **136**, 1–51.

13 T. T. Ashburn and K. B. Thor, Drug repositioning: identifying and developing new uses for existing drugs, *Nat Rev Drug Discov*, 2004, **3**(8), 673–683.

14 S. Katharios-Lanwermeyer, G. B. Whitfield, P. L. Howell and G. A. O'Toole, Pseudomonas aeruginosa Uses c-di-GMP Phosphodiesterases RmcA and MorA To Regulate Biofilm Maintenance, *mBio*, 2021, **12**(1), e03384.

15 Y. Xia, X. Wei, P. Gao, C. Wang, A. de Jong, J. H. K. Chen, *et al.*, Bismuth-based drugs sensitize Pseudomonas aeruginosa to multiple antibiotics by disrupting iron homeostasis, *Nat Microbiol.*, 2024, **9**(10), 2600–2613.

16 S. Qin, W. Xiao, C. Zhou, Q. Pu, X. Deng, L. Lan, *et al.*, Pseudomonas aeruginosa: pathogenesis, virulence factors, antibiotic resistance, interaction with host, technology advances and emerging therapeutics, *Signal Transduction Targeted Ther.*, 2022, **7**(1), 199.

17 A. L. Spoering and K. Lewis, Biofilms and Planktonic Cells of *Pseudomonas aeruginosa* Have Similar Resistance to Killing by Antimicrobials, *J. Bacteriol.*, 2001, **183**(23), 6746–6751.

18 M. Gallego, X. Pomares, M. Espasa, E. Castañer, M. Solé, D. Suárez, *et al.*, Pseudomonas aeruginosa isolates in severe chronic obstructive pulmonary disease: characterization and risk factors, *BMC Pulm. Med.*, 2014, **14**(1), 103.

19 I. J. Schalk and L. Guillon, Pyoverdine biosynthesis and secretion in *Pseudomonas aeruginosa*: implications for metal homeostasis, *Environ. Microbiol.*, 2013, **15**(6), 1661–1673.

20 G. Ghssein and Z. Ezzeddine, A Review of Pseudomonas aeruginosa Metallophores: Pyoverdine, Pyochelin and Pseudopaline, *Biology*, 2022, **11**(12), 1711.

21 A. Sánchez-Jiménez, F. J. Marcos-Torres and M. A. Llamas, Mechanisms of iron homeostasis in *Pseudomonas aeruginosa* and emerging therapeutics directed to disrupt this vital process, *Microb. Biotechnol.*, 2023, **16**(7), 1475–1491.

22 A. Sánchez-Jiménez, F. J. Marcos-Torres and M. A. Llamas, Mechanisms of iron homeostasis in *Pseudomonas aeruginosa* and emerging therapeutics directed to disrupt this vital process, *Microb. Biotechnol.*, 2023, **16**(7), 1475–1491.

23 A. Firoz, M. Haris, K. Hussain, M. Raza, D. Verma, M. Bouchama, *et al.*, Can Targeting Iron Help in Combating Chronic Pseudomonas Infection? A Systematic Review, *Cureus*, 2021, **13**(3), e13716.

24 Y. Zhang, X. Pan, L. Wang and L. Chen, Iron metabolism in *Pseudomonas aeruginosa* biofilm and the involved iron-targeted anti-biofilm strategies, *J. Drug Target.*, 2021, **29**(3), 249–258.

25 K. Vadakkan, K. Sathishkumar, V. O. Mapranathukaran, A. K. Ngangbam, B. D. Nongmaithem, J. Hemapriya, *et al.*, Critical review on plant-derived quorum sensing signaling inhibitors in pseudomonas aeruginosa, *Bioorg. Chem.*, 2024, **151**, 107649.

26 B. Sırıken, V. Öz and İ. Erol, Quorum sensing systems, related virulence factors, and biofilm formation in Pseudomonas aeruginosa isolated from fish, *Arch. Microbiol.*, 2021, **203**(4), 1519–1528.

27 A. Kar, L. Giri, G. Kenguva, S. R. Rout and R. Dandela, Mechanical approach for creating different molecular adducts and regulating salt polymorphs: a case study of the anti-inflammatory medication ensifentrine, *RSC Mechanochem.*, 2024, **1**(5), 437–446.

28 A. Kar, L. Giri, G. Kenguva, S. R. Rout and R. Dandela, Polymorphism, phase transition, and physicochemical property investigation of Ensifentrine, *CrystEngComm*, 2024, **26**(28), 3783–3790.

29 M. J. A. Walker, B. M. C. Plouvier, J. S. Northen and P. Fernandes, *Crystalline form of pyrimido [6,1-A] isoquinolin-4-one compound*, 2015, vol. 2, 12.

30 P. L. Spargo, *New Compound and Process*, 2018.

31 A. Kar, L. Giri, G. Kenguva, S. R. Rout and R. Dandela, Polymorphism, phase transition, and physicochemical property investigation of Ensifentrine, *CrystEngComm*, 2024, **26**(28), 3783–3790.

32 A. Kar, L. Giri, G. Kenguva, R. Rout S and R. Dandela, Mechanical approach for creating different molecular adducts and regulating salt polymorphs: a case study of the anti-inflammatory medication ensifentrine, *RSC Mechanochem.*, 2024, **1**(5), 437–446.

33 M. Hema, S. A. Princy, V. Sridharan, P. Vinoth, P. B. P. Balamurugan and M. N. Sumana, Synergistic activity of quorum sensing inhibitor, pyrizine-2-carboxylic acid and antibiotics against multi-drug resistant V. cholerae, *RSC Adv.*, 2016, **6**(51), 45938–45946.

34 B. Kim, J. S. Park, H. Y. Choi, S. S. Yoon and W. G. Kim, Terrein is an inhibitor of quorum sensing and c-di-GMP in Pseudomonas aeruginosa: a connection between quorum sensing and c-di-GMP, *Sci. Rep.*, 2018, **8**(1), 8617.

35 K. S. Musthafa, B. S. Sivamaruthi, S. K. Pandian and A. V. Ravi, Quorum Sensing Inhibition in Pseudomonas aeruginosa PAO1 by Antagonistic Compound Phenylacetic Acid, *Curr. Microbiol.*, 2012, **65**(5), 475–480.

36 R. Shobana, J. H. Thahirunnisa, S. Sivaprakash, A. J. Amali, A. P. Solomon and D. Suresh, Effect of palladium(II) complexes on NorA efflux pump inhibition and resensitization of fluoroquinolone-resistant Staphylococcus aureus: *in vitro* and *in silico* approach, *Front. Cell. Infect. Microbiol.*, 2024, **15**, 13.